Civil Engineering Infrastructures Journal, 52(2): 205 – 224, December 2019
Print ISSN: 2322-2093; Online ISSN: 2423-6691
DOI: 10.22059/ceij.2019.257833.1484

Performance of Nondestructive Sonic Echo Testing Method on Partially Dismantled Unknown Wood Bridge Foundations; A Case Study

Rashidyan, S.[1*], Maji, A.[2] and Ng, T.T.[3]

[1] Senior Lecturer, Department of Engineering Technology, University of North Texas, Denton, Texas, USA.
[2] Professor Emeritus, Civil Engineering Department, University of New Mexico, Albuquerque, NM, USA.
[3] Professor, Civil Engineering Department, University of New Mexico, Albuquerque, NM, USA.

Received: 13 May 2018; Revised: 29 May 2019; Accepted: 30 Sep. 2019

ABSTRACT: Sonic Echo (SE) testing method is a well-known, versatile method to gather information pertaining to unknown bridge foundations. Many studies on the applicability and methodology improvement of SE tests to evaluate individual piles and foundations supporting the superstructure have been reported previously. However, there is a rare opportunity for obtaining the performance of SE tests without the bridge deck. In the current study, three piles of a dismantled unknown bridge foundation were tested. Unusual vibrations on velocity signals were found which are independent of the location of the sensors. Such signals do not contain identifiable echoes from the pile toe. Therefore, they cannot be used to determine the depth of the piles. The results and observations of this study show that there is little future application for conducting SE tests on bridges that are out of service.

Keywords: Foundation, Nondestructive, Pile, Sonic Echo, Wood.

INTRODUCTION

Unknown bridge foundations may be vulnerable to scour. Thus, in order to determine scour risk, it is important to assess the characteristics of such foundations, particularly the type and depth of foundations. Conventional excavation methods used to evaluate unknown bridge foundations, such as coring and boring, are expensive, destructive, and limited in their application. Many nondestructive testing (NDT) technologies have been purposed and utilized to assess the condition of civil infrastructure and materials (Briaud et al., 2002; Chidambarathanu, 2019; Ghasemzadeh and Abounouri, 2013; Lai et al., 2012; Rashidyan et al., 2019). Among common NDT methods, the Sonic Echo (SE) method is a well-known, economical method which can be used to collect the specifications of unknown bridge foundations.

The SE Test is performed based on the principle of longitudinal wave propagation in long rods.

Consider the free vibration of an infinitely long rod with cross sectional area, A, Young's modulus E, Poisson's ratio *v*, and

* Corresponding author E-mail: srashidyan@yahoo.com

density ρ, as shown in Figure 1 (Kramer, 1996). As stress wave travels along the rod and passes through the small element shown in Figure 1, axial stresses are generated on the left and right edges of the element. The dynamic equilibrium of the element requires that

$$\left(\sigma_{x_0} + \frac{\partial \sigma_x}{\partial x}\,dx\right)A - \sigma_{x_0}\,A = \rho A dx\,\frac{\partial^2 u}{\partial t^2} \quad (1)$$

Simplifying this equation will yield the one-dimensional equation of motion:

$$\frac{\partial \sigma_x}{\partial x} = \rho\frac{\partial^2 u}{\partial t^2} \quad (2)$$

For linear elastic materials, $\sigma_x = E\varepsilon_x$, the equation becomes:

$$\frac{\partial^2 u}{\partial t^2} = v^2\,\frac{\partial^2 u}{\partial x^2} \quad (3)$$

where *v*: is the wave propagation velocity; for this case the wave travels at $v = \sqrt{E/\rho}$.

In SE Test, the abovementioned longitudinal waves are generated by striking the pile head with a hammer as indicated in the SE tests setup depicted in Figure 2 (Hertlein and Davis, 2007). Upon striking, a longitudinal wave with velocity *v* is generated along the pile. The generated wave travels down with velocity *v* and reaches to the bottom of the pile. When the incident wave reaches the pile-soil interface, due to the change in impedance (Z = *EA/v*) of the materials, part of its energy will be transmitted through the interface to continue traveling in the soil (transmitted wave) and the remainder will be reflected at the interface toward the top of the pile as indicated in Figure 3. The impedance changes can be as a result of change in pile section, concrete density or pile–soil properties.

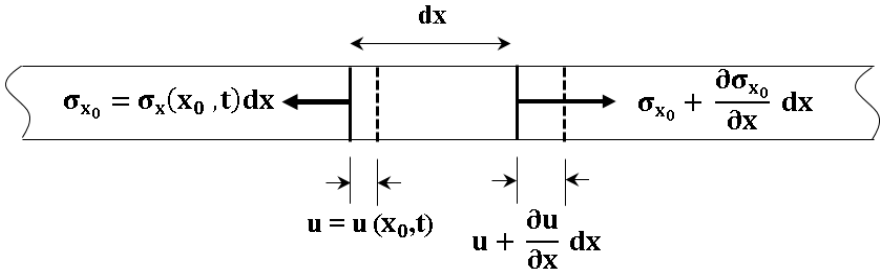

Fig. 1. Stresses and displacements at ends of element of length dx and cross-sectional area, A. (Kramer, 1996)

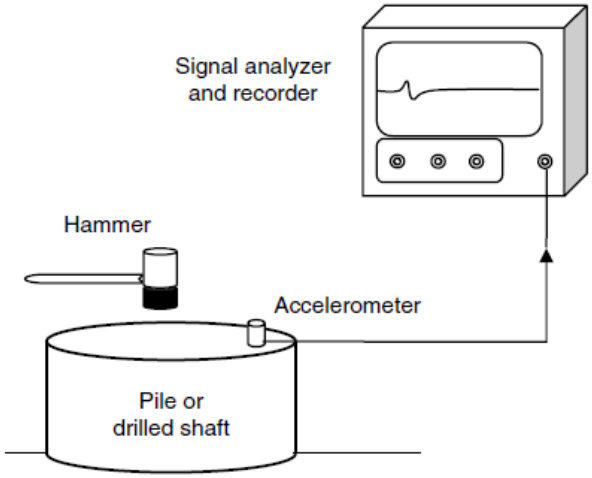

Fig. 2. Schematic of the SE test set-up (Hertlein and Davis, 2007)

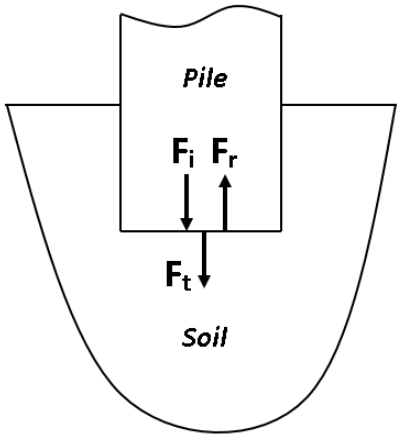

Fig. 3. Incident (Fi), reflected (Fr) and transmitted (Ft) waves at the pile-soil interface

The reflected and transmitted waves are correlated to the incident wave at pile toe:

$$F_t = F_i \left(\frac{2\,Z_s}{Z_s + Z_p} \right) \quad (4a)$$

$$F_r = F_i \left(\frac{Z_{s-} Z_p}{Z_s + Z_p} \right) \quad (4b)$$

Using a sensor (accelerometer or geophone velocity transducer) coupled to the pile head (see Figure 2), the time lapse, t, between the hammer impulse and the arrival of the reflected waves at the pile head from pile tip is then measured. A typical example of a Sonic Echo velocity (signal)–time response plot is indicated in Figure 4 (Hertlein and Davis, 2007).

The distance traveled by the stress wave, will be the product of time lapse *t* between the impulse and echo and propagated wave velocity *v*. This distance is twice of the pile length when the sensor is placed at the top of the pile. Finally, the length of the pile, L, can be calculated:

$$L = \frac{v \times t}{2} \quad (5)$$

The SE method was initially used to evaluate the condition of bored cast-in situ and pre-cast driven piles (Rausche and Goble, 1979; Weltman, 1977). The method was then improved and modified to evaluate the characteristics of unknown bridge foundations supporting bridge decks (Chai and Phoon, 2012; Huang and Chen, 2007; Rashidyan et al., 2016). In performing SE tests on such piles supporting bridge decks, the schematic SE test set up indicated in Figure 5 can be used to determine the depth of the piles. Knowing the propagated wave velocity, the total and buried lengths of the pile can be calculated.

$$L_{tr} = \frac{v \times \Delta t}{2} \quad (6a)$$

$$L_{total} = L_{tr} + L_a \quad (6b)$$

$$L_b = L_{total} - L_e \quad (6c)$$

where L_{tr}: is distance between the sensor location and pile toe, L_{total}: is total length of pile, L_b: is buried length of pile, Δt: is time difference between the impulse and first echo and *v*: is propagated wave velocity.

As previously mentioned, many studies on the applicability and methodology improvement of SE tests to evaluate the characteristics of unknown bridge foundations have been reported. They have discussed the individual piles without superstructure as well as field and numerical studies on piles and piers underneath pile caps (Rashidyan et al., 2017; White et al., 2008).

In the current study, the performance of SE tests on dismantled bridge foundations is discussed. Such foundations may exist in

cases where either the bridge deck or the entire bridge is supposed be replaced. The investigated bridge was a bridge which was supposed to be demolished and replaced due to high level of susceptibility to scour. At the time of testing, only the foundation comprising pile cap and piles were available, and the bridge deck had already been removed. Before destructing the foundation, SE tests were performed on this foundation and the obtained signals were investigated to examine whether the SE testing method is a proper method to assess the characteristics of such foundation.

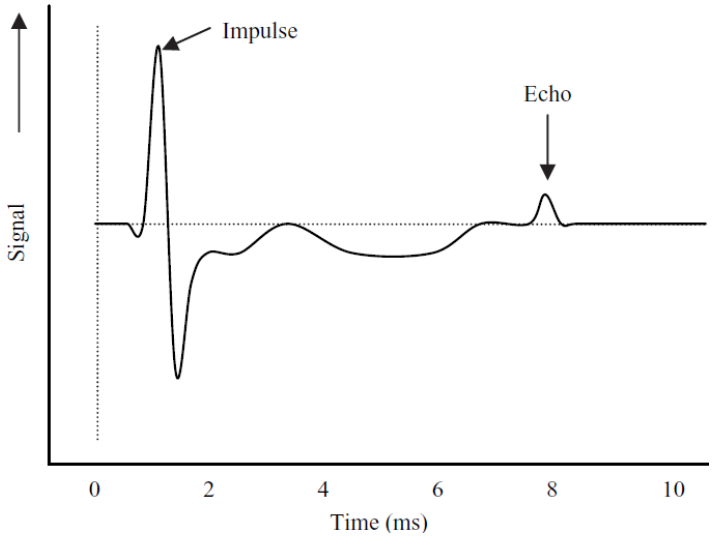

Fig. 4. A typical example of a Sonic-Echo velocity (signal)–time response plot (Hertlein and Davis, 2007)

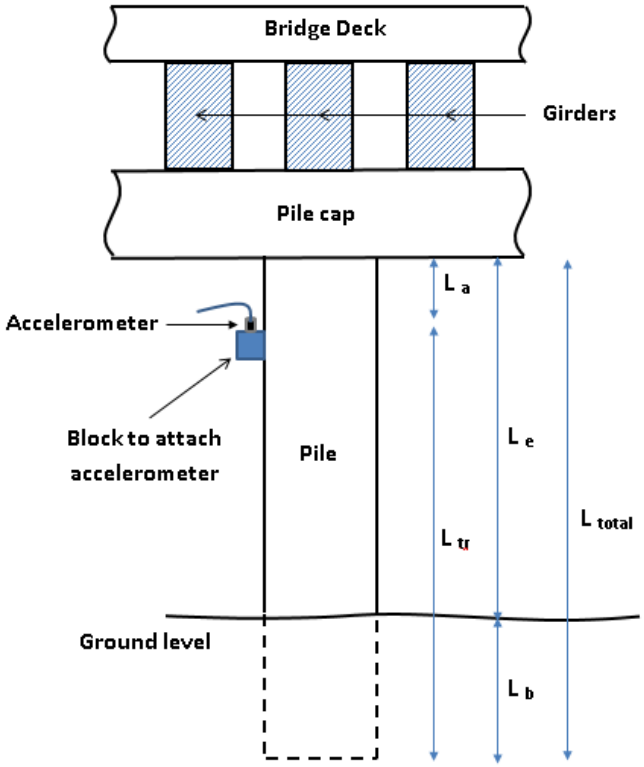

Fig. 5. A typical Sonic Echo/Impulse Response test setup for wood piles supporting bridge decks

METHODOLOGY

To achieve the goals of this research, SE tests were carried out on three timber piles of a partially dismantled highway bridge. The bridge was located 103 km east of Las Vegas, New Mexico, USA, on Route 419. The New Mexico Department of Transportation (NMDOT) had already removed the bridge deck since this bridge was supposed to be replaced due to its susceptibility to scour. Therefore, only the piles and the pile cap existed at the time of testing. The piles were eventually pulled out and a new bridge was constructed. The street view and the foundation plan are shown in Figure 6.

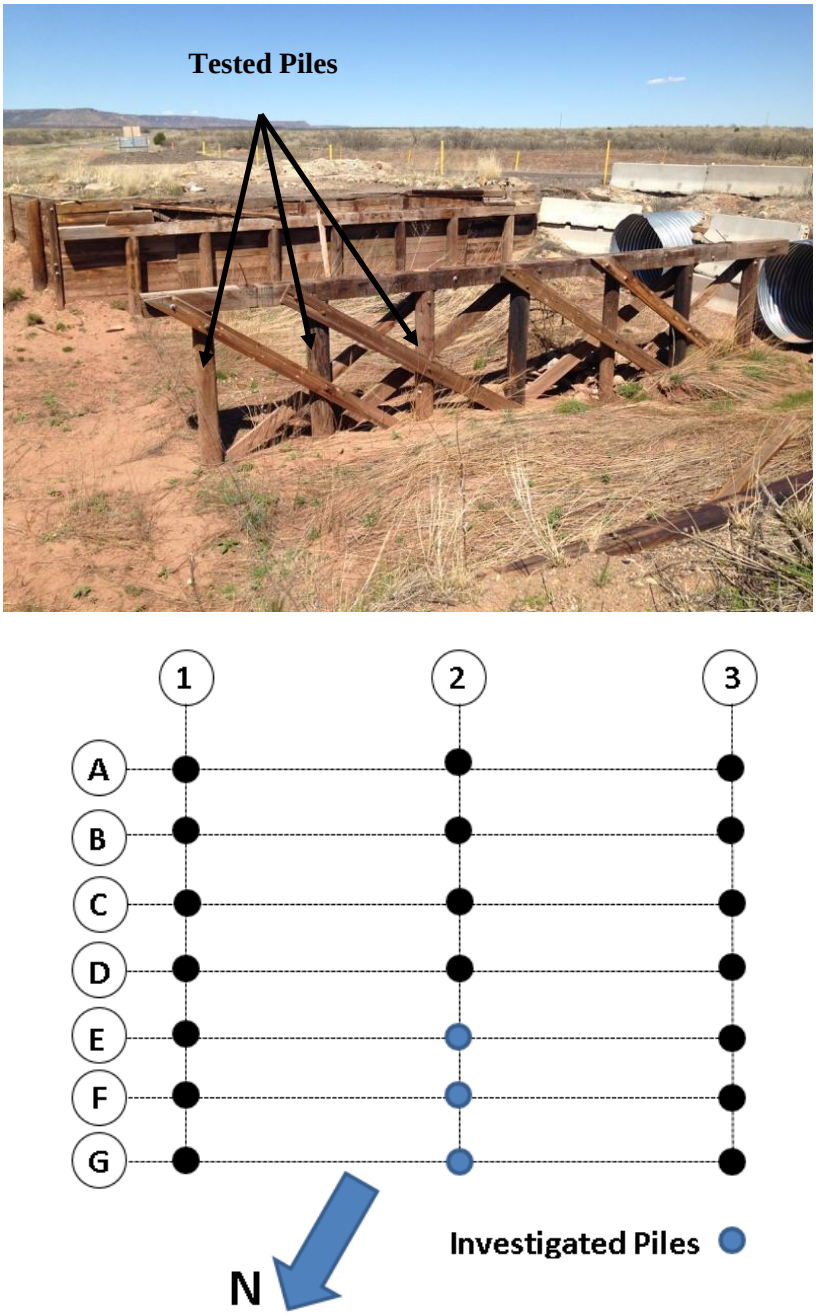

Fig. 6. a) Photo and b) investigated piles; of the partially dismantled bridge on Route 419

SE test procedure was followed step by step in conducting the field tests:

Striking and Receiver Setup

Numerous SE tests were performed by striking a hammer on the foundation. Depending on the accessibility of the pile top, different striking methods can be used to generate sonic waves along the pile. In this research, striking methods such as central and eccentric vertical striking on top surface of pile cap, and upward vertical striking on the bottom surface of pile cap were examined. The effect of striking method on the obtained signals was investigated. It should be noted that the downward strikes generate compressive waves, whereas upward strikes impart tensile waves into the piles. Since the piles' tops were not accessible, the accelerometers were mounted vertically on wooden blocks attached to the side of the test pile with glue. The SE tests setup including the locations of the striking points (black solid points) and accelerometers for each pile are indicated in Figure 7. Downward striking on the top surface and upward striking on the bottom surface of the pile cap were used for piles G-2 (Points A to L) and E-2 (Points Q to X). Only downward striking on the top surface of the pile cap was applied for Pile F-2 (Points M to P). The distances between adjacent striking points (black solid circles) were 7.5 cm. Points L and U (Figures 7a and 7c) are also located 7.5 cm from the pile edge. As indicated in Figure 7, two accelerometers were also used to measure the depth of each pile.

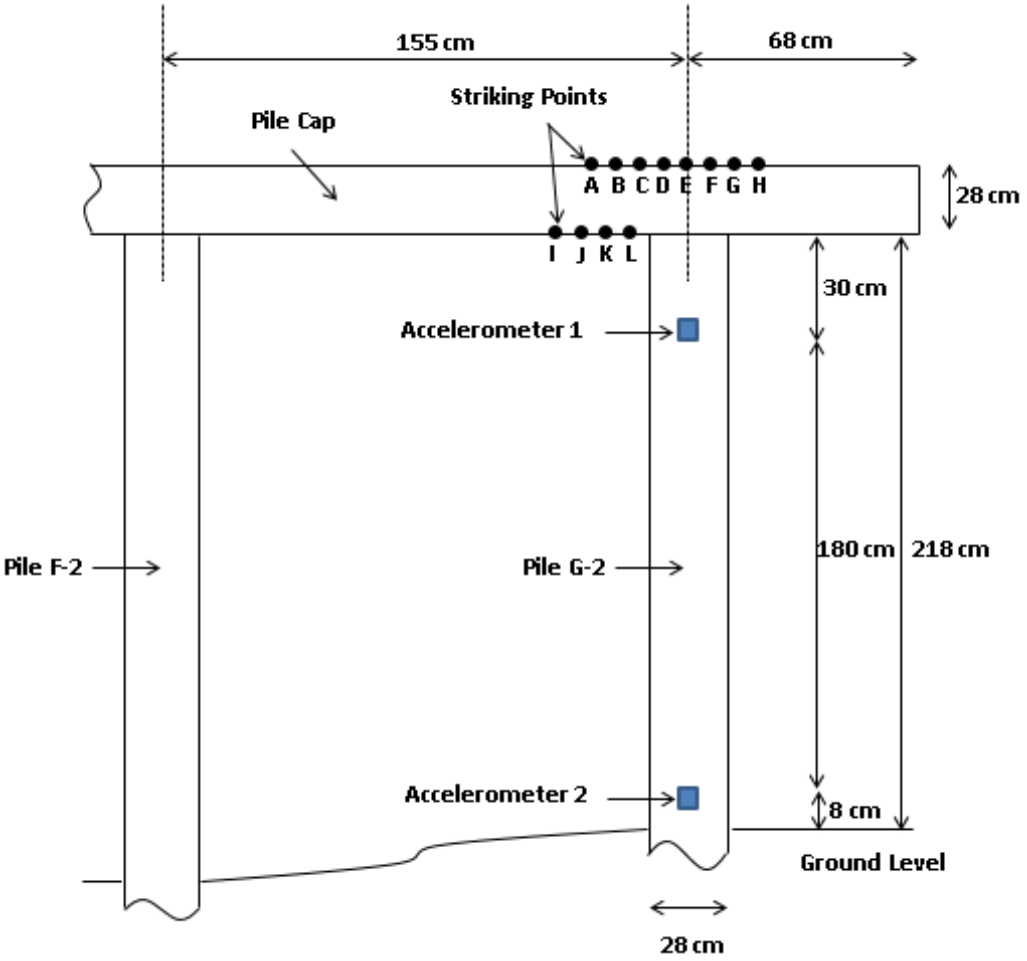

(a)

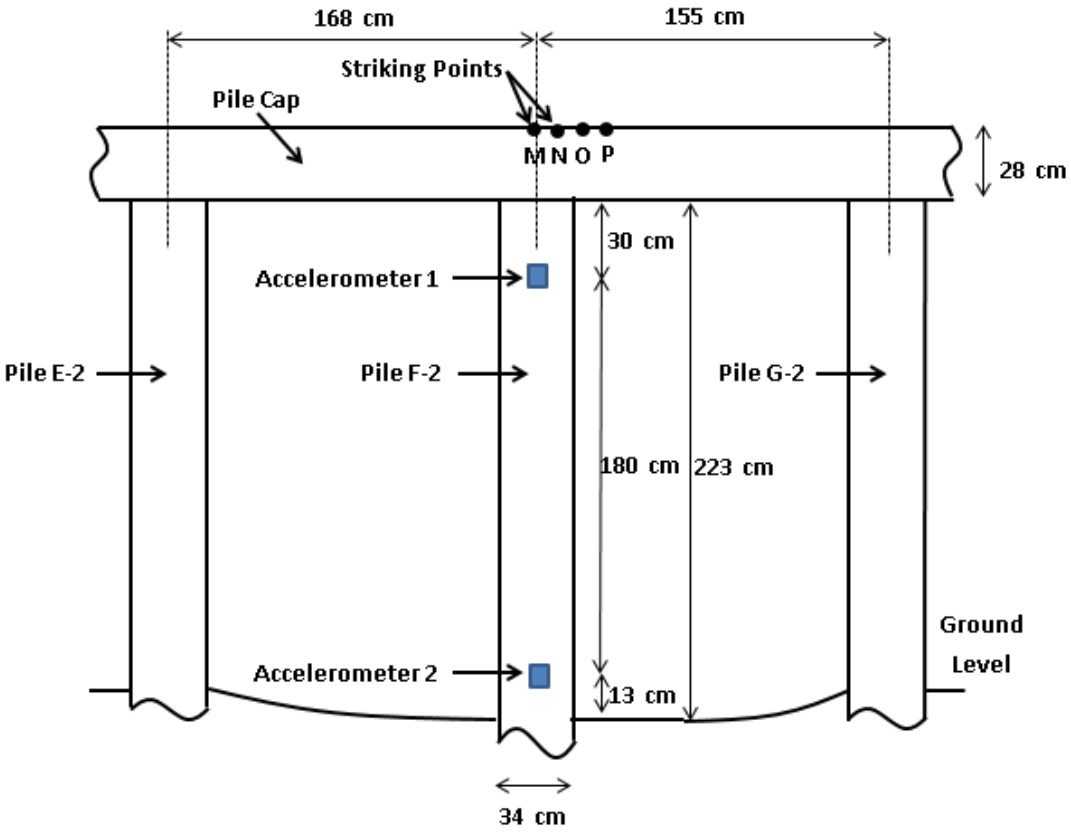

(b)

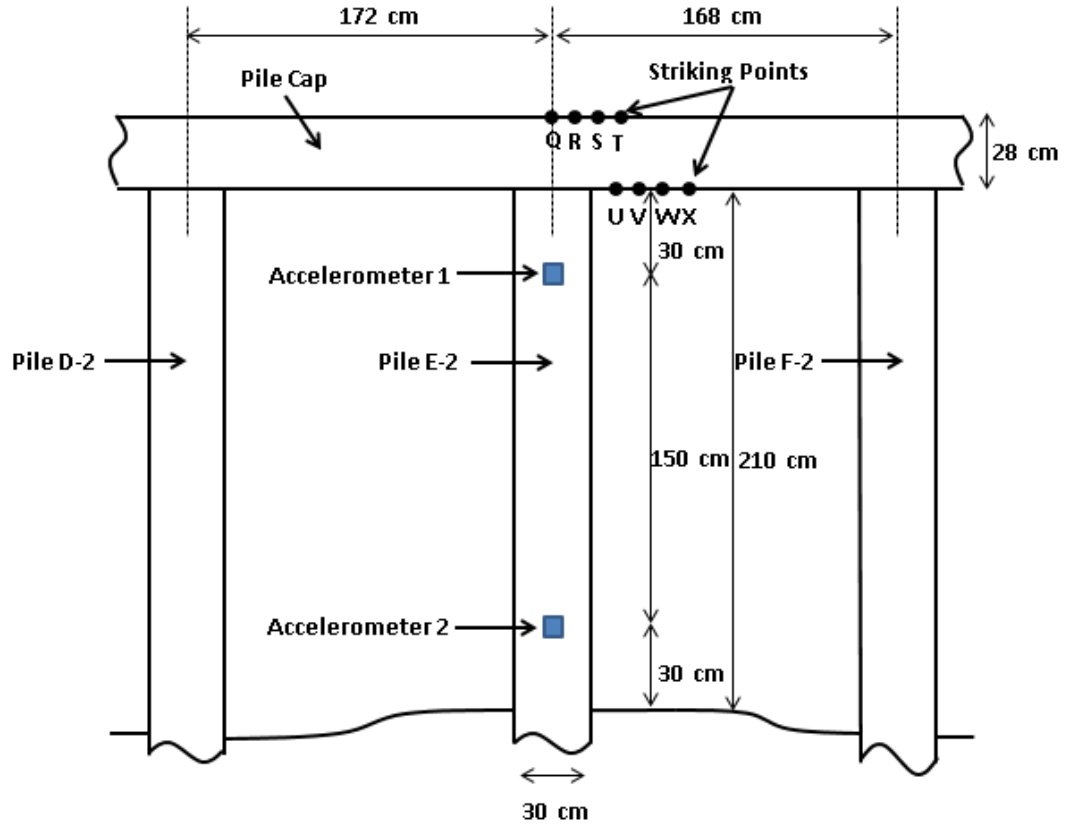

(c)

Fig. 7. SE test setup for piles: a) G-2, b) F-2 and c) E-2

Hardware Assembly and Data Acquisition

The utilized equipment, Freedom Data PC (FDPC) was acquired pursuant to ASTM D5882-07-2013 (American Society for Testing Materials, 2013) and ACI 228.2R-13 (American Concrete Institution, 2013). The FDPC provides the user with flexibility for stress-wave based NDT condition evaluation of different type of materials. Two 100mv/g accelerometers, and an instrumented hammer were also used to conduct the tests.

Data Processing

The velocity amplitude-time graphs obtained from the accelerometers were investigated to determine the pile lengths by using Eq. (6). The mechanical properties of the utilized wood material (Southern Pike) were obtained from national design specification for wood construction (American Wood Council, 2018):

Modulus of Elasticity: E = 1,054,600,000 N/m^2 (1,500,000 psi)

Specific Gravity G_s = 0.55

Poisson's ratio μ = 0.328 (United States Department of Agriculture Forest Service, 2010)

Using the abovementioned values, the propagated wave velocity is calculated.

$$v = \sqrt{\frac{E}{\rho}} = \sqrt{\frac{105406000 \times 9.81}{0.55 \times 1000}} = 4337\ m/s$$

OBSERVATIONS AND DISCUSSION

Pile G-2

A SE Test was performed on Pile G-2 by striking point E (see Figure 7a). The results of the SE test by striking point E is elaborated here since the results of other tests contain similar interfering variables. Point E is located on the pile axis. The velocity signals obtained from accelerometers 1 and 2 are indicated in Figure 8. This figure shows clear impulses (blue arrows) and multiple consecutive valleys (black arrows) for both accelerometers. The time lapses between the first four valleys (Δt_1, Δt_2 and Δt_3**)** are indicated in Table 1.

Table 1. Time lapses between the first four valleys for tests conducted by striking on point E

Accelerometer	Δt_1 (μs)	Δt_2 (μs)	Δt_3 (μs)
1	2160	2140	2080
2	2100	2000	2000

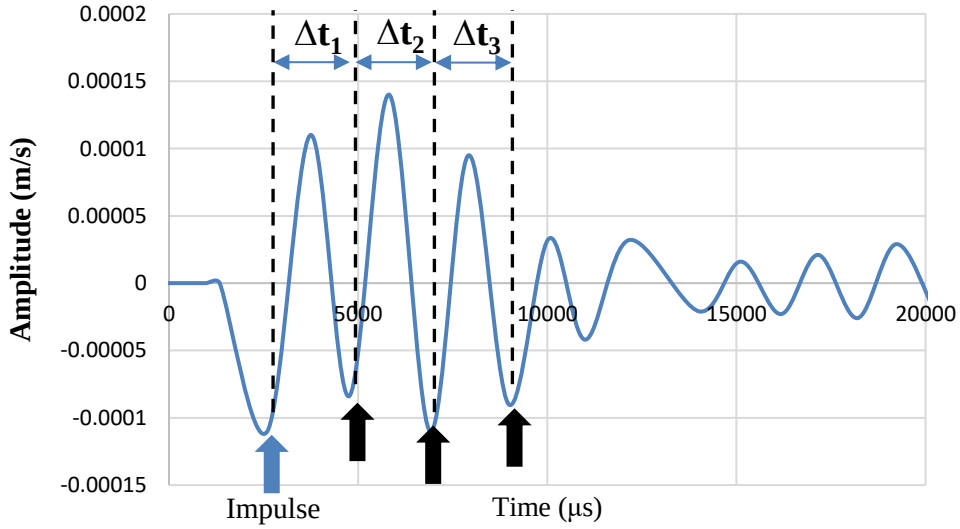

(a)

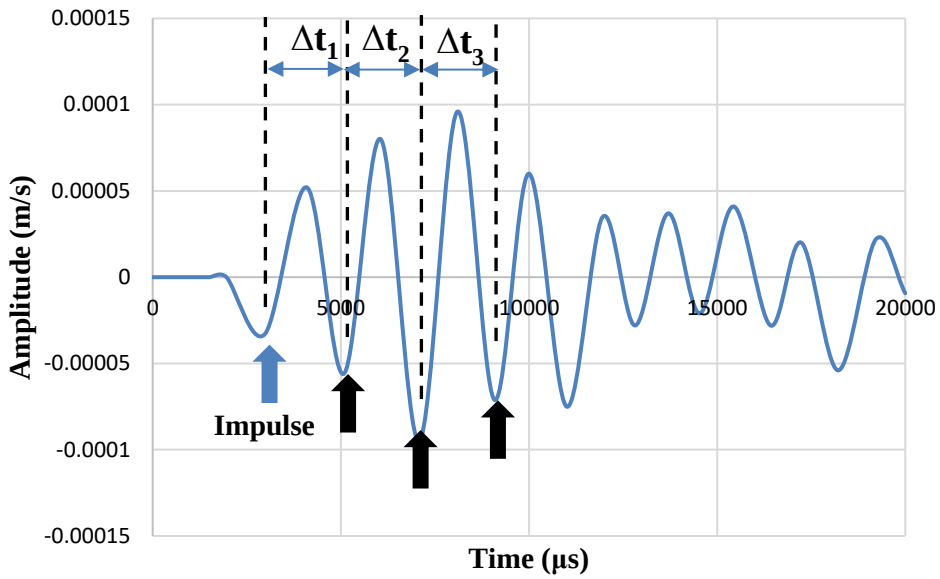

(b)

Fig. 8. Velocity signals obtained from: a) Accelerometer 1 and b) Accelerometer 2, for Pile G-1 by vertical downward strikes on the center of the top surface of the pile cap (Point E)

In Figure 8a, the time difference between the impulse and successor valley is 2160 µs. By substituting this number in Eq. (6), the corresponding distance between the accelerometer 1 and expected pile toe (L_b) can be calculated:

$$L_{tr} = \frac{v \times \Delta t}{2} = \frac{4337 \times 2160 \times 10^{-6}}{2} = 4.68 \text{ m}$$

$$L_b = 4.68 - 1.88 = 2.8 \text{ m}$$

It shows that the embedment of the pile is only 2.8 m. However, this calculated length does not seem to be the actual buried length of the pile for the following reasons:

First, the consecutive echoes (black arrows) have large amplitudes not significantly smaller than the impulse and a decaying trend of amplitudes is not seen on the graph. This conflicts with the SE test theory. Based on the principals of the SE method (Davis, 1995), the amplitudes should decay due to the effect of material and surrounding soil energy damping. Therefore, the consecutive valleys do not seem to be the reflections from the pile toe.

Second, the time difference between the impulse and next consecutive valley on the signal obtained from accelerometer 2 is equal to 2100 µs. This number is very close to the time lapse between the impulse and the next valley from accelerometer 1 (2160 µs). The time lapse obtained from accelerometer 1 is only 60 µs larger than the time lapse from accelerometer 2. This implies that both accelerometers show approximately equal distances between the accelerometer location and the expected pile toe. This cannot be true. There is a 1.8 m distance between the two accelerometers (see Figure 7a) and the time difference between accelerometers 2 and 1 should be 830 µs (2×1.8/4337 µs). Since the measured time difference (60 µs) is significantly smaller than the expected time difference (830 µs), the first valley following the impulse does not seem to be the echo from the pile toe. The results do not vary for different sensor locations. Therefore, such vibrations seem to be from other sources other than the pile toe.

Finally, the time lapses Δt_2 and Δt_3 are very close to Δt_1 in both accelerometers. In accelerometer 1, Δt_2 and Δt_3 are smaller than Δt_1 for only 0.9 and 3.7 percent respectively.

In accelerometer 2, both Δt_2 and Δt_3 are 4.8 percent smaller than Δt_1. The vibration is harmonic. Such vibrations are not from the wave travels between the top and bottom of the pile. For instance, in accelerometer 2, the distance between the accelerometer and pile top is 2.10 m. This means the when the reflected wave from the pile toe passes through this accelerometer it needs 968 µs ($2\times2.1\times10^6$ / 4337 µs) to be sensed again after reflecting from the pile top. However, the difference between the second and third valley on the graph is 2000 µs which is more than twice of the expected travel duration (968 µs).

More SE tests were performed on Pile G-2 by downward strikes applied on the left (Points A to D) and right sides (F to H) of Point A. Upward striking on points I to L (bottom surface of the pile cap) were also examined. The signals obtained from downward strikes on the right and left sides of point A, and upward strike on the bottom surface of pile cap are indicated in Figures 9 to 11. The measured time lapses Δt_1, Δt_2 and Δt_3 are also indicated in Tables 2 to 4. It should be noted that Δt_1, Δt_2 and Δt_3 are the time lapses between consecutive valleys as previously defined in Figure 8.

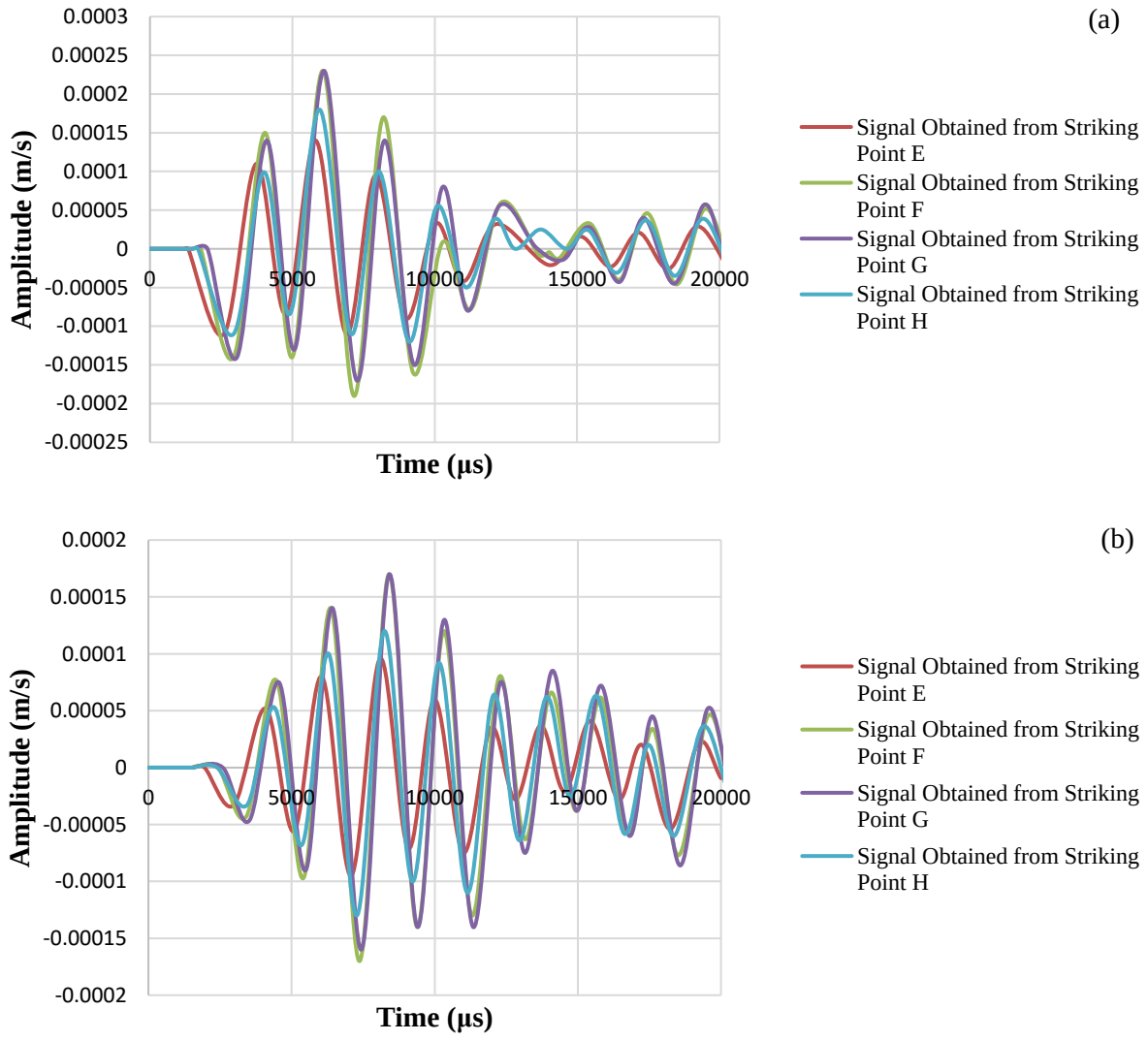

Fig. 9. Signals obtained from downward strikes on points E to H for: a) Accelerometer 1 and b) Accelerometer 2

Table 2. Time lapses between the first four valleys for tests conducted by striking points E to H

Striking point	Accelerometer	Δt_1 (μs)	Δt_2 (μs)	Δt_3 (μs)
E	1	2160	2140	2080
	2	2100	2000	2000
F	1	2060	2160	2080
	2	2000	1960	2000
G	1	2020	2180	2020
	2	1960	1940	1960
H	1	1980	2140	2040
	2	1920	1920	1940

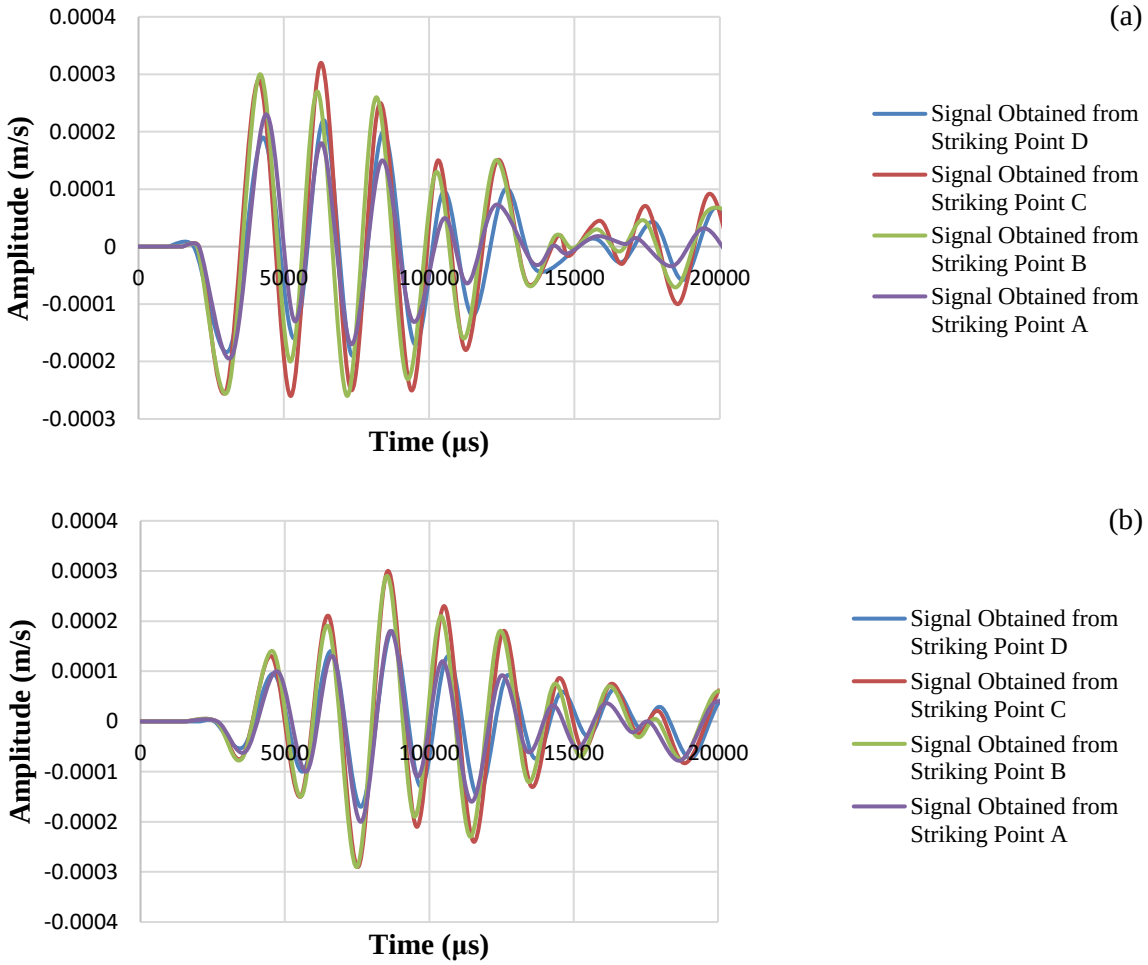

Fig. 10. Signals obtained from downward strikes on points A to D for: a) Accelerometer 1 and b) Accelerometer 2

Table 3. Time lapses between the first four valleys for tests conducted by striking points A to D

Striking point	Accelerometer	Δt_1 (μs)	Δt_2 (μs)	Δt_3 (μs)
D	1	2240	2000	2140
	2	2060	2020	2060
C	1	2220	2080	2060
	2	2020	2000	2020
B	1	2140	1960	2060
	2	2040	1940	1980
A	1	2160	1940	2120
	2	2100	1900	1940

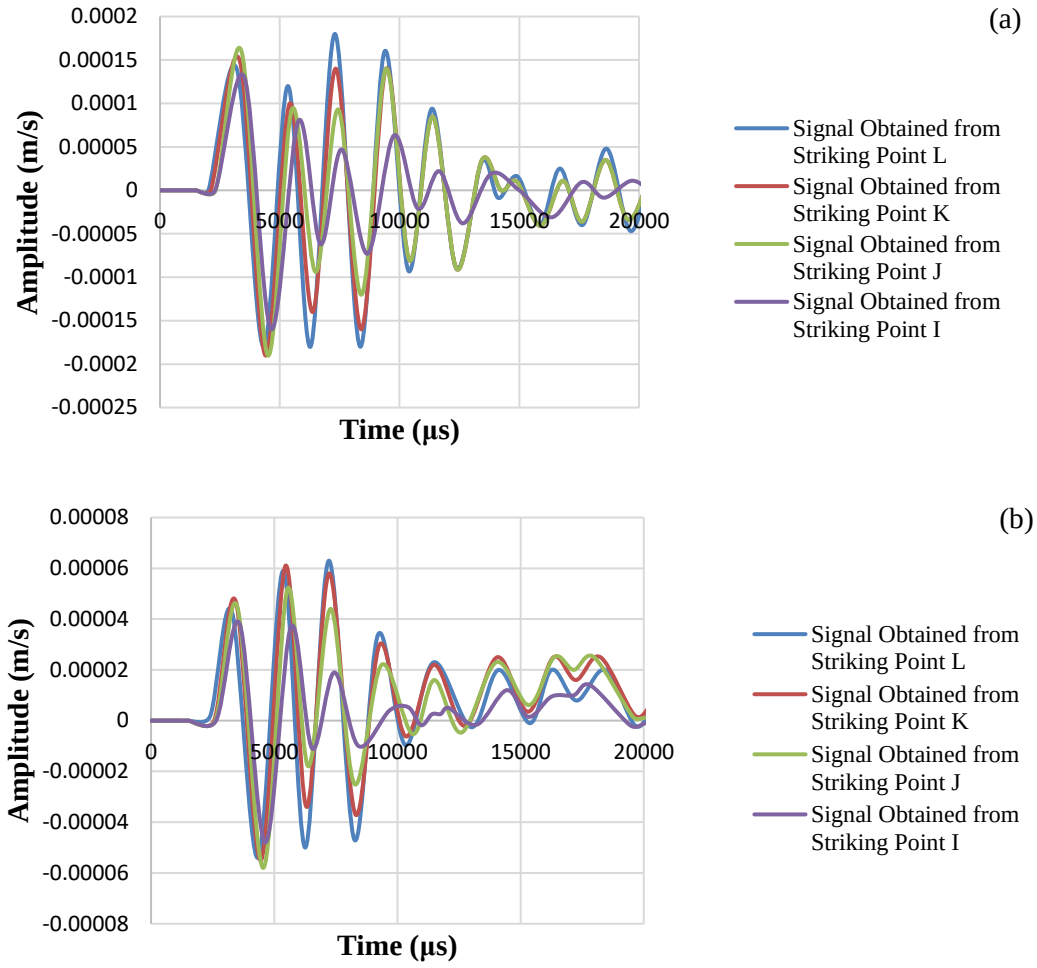

Fig. 11. Signals obtained from downward strikes on points L to I for: a) Accelerometer and b) Accelerometer 2

Table 4. Time lapses between the first four valleys for tests conducted by striking points L to I

Striking point	Accelerometer	Δt_1 (µs)	Δt_2 (µs)	Δt_3 (µs)
L	1	2140	1960	2080
	2	2080	1860	2000
K	1	2100	1920	2100
	2	2020	1780	2040
J	1	2120	1920	2000
	2	2040	1760	2060
I	1	2260	1800	2180
	2	2080	1760	2240

The graphs indicated in Figures 9 and 10 show that vibrations with patterns similar to Figure 8 occur in all tests. The results obtained from the upward strikes show the same pattern although the signals are flipped compared to the downward strikes. It should be noted that downward strikes impart compressive waves in to the pile, whereas the upward strikes generate tensile waves. In signals indicated in Figures 9 to 11, the vibrations have large amplitudes which do not decay fast with time. In addition, the consecutive vibrations have similar durations. The average durations Δt_1, Δt_2 and Δt_3 are summarized in Table 5.

Table 5. Average time lapses between the first four valleys for tests conducted by striking points A to L

Striking points	Accelerometer	Average Δt_1 (µs)	Average Δt_2 (µs)	Average Δt_3 (µs)
E to H	1	2050	2155	2055
	2	1995	1955	1975
A to D	1	2190	1995	2095
	2	2055	1965	2000
I to L	1	2155	1900	2090
	2	2055	1790	2085
Average		2083	1960	2050

The results indicated in Table 5 show that the average lapses between the impulse and the next valley (Average Δt_1) for accelerometer 1 is very close to that of obtained from accelerometer 2. The differences between the time lapses obtained from accelerometers 1 and 2 are 55, 135 and 100 µs for tests E to H, A to D, and I to L respectively. These values are much smaller than 830 µs which was expect based on the 1.8 m distance between the two accelerometers. Thus, the obtained signals are independent of the location of the sensors on the piles and both show approximately the same buried lengths. In addition, the location and direction of the strikes do not affect the results. The results also show that the durations of the consecutive vibrations are very close to each other. They are 2083, 1960 and 2050 µs for the first, second and third vibrations respectively. The average of second and third vibrations are only 5.9 and 1.6% smaller than the average duration of the first echo respectively.

Pile F-2

SE tests were conducted on pile F-2 using downward strikes on the top surface of the pile. The obtained signals from accelerometers 1 and 2 are indicated in Figure 12. The graphs show similar vibration pattern as pile G-2. However, the signals obtained from accelerometer 2 seem more disturbed compared to accelerometer 1. Therefore, only the time differences between the impulse and next valley are indicated in Table 6. The results indicated in Table 6 show that the time lapses between accelerometers 1 and 2 are significantly smaller than 830 µs (2×1.8/4337 µs) which is expected to be measured since the accelerometer 1 is 1.8 m away from accelerometer 2. Therefore, it is not probable that the valley following the impulse represents the echo from pile bottom.

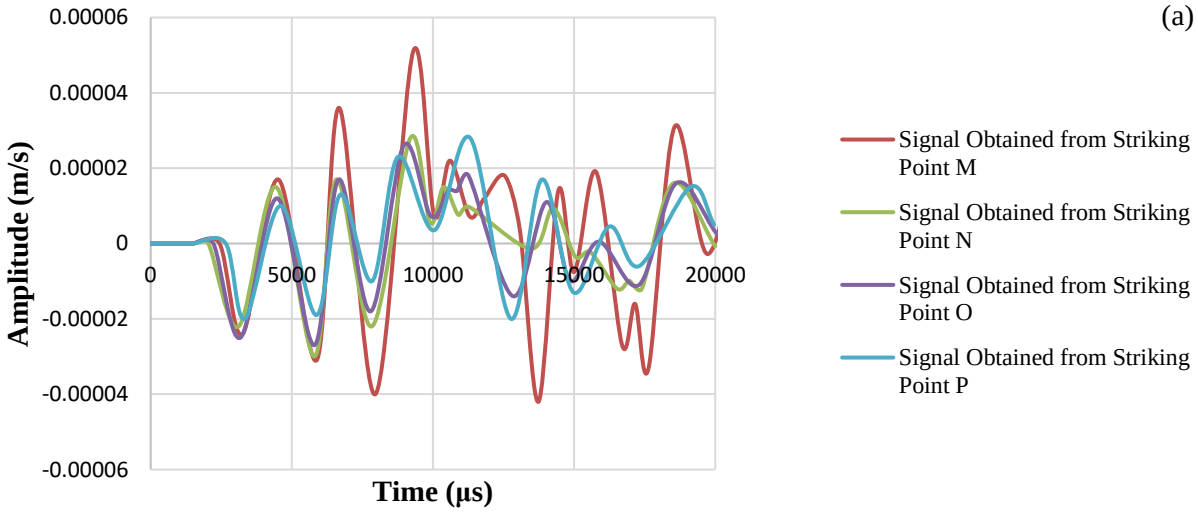

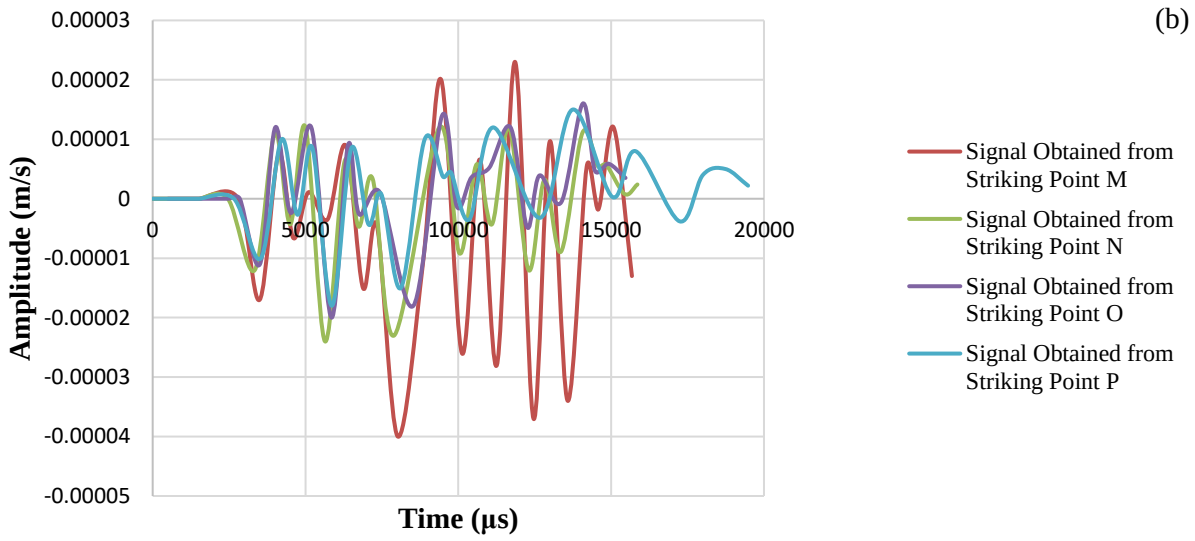

Fig. 12. Signals obtained from downward strikes on points M to P for: a) Accelerometer 1 and b) Accelerometer 2

Table 6. Time difference between the impulse and first valley for tests conducted by striking points M to P

Test	Accelerometer	Δt_1 (µs)	Time lapse between accelerometers 1 and 2 (µs)
M	1	2620	400
	2	2220	
N	1	2680	380
	2	2300	
O	1	2620	280
	2	2340	
P	1	2540	220
	2	2320	

Pile E-2

SE tests were also conducted on pile E-2 using downward strikes on the top surface of the pile and upward strikes on the bottom surface of the pile cap based on the setup previously indicated in Figure 7c. The obtained signals from accelerometers 1 and 2 are indicated in Figures 13 and 14. Again, the graphs show similar vibration pattern as piles G-2 and F-2. The Δt_1, Δt_2 and Δt_3 are indicated in Tables 7 and 8 for both downward and upward strikes.

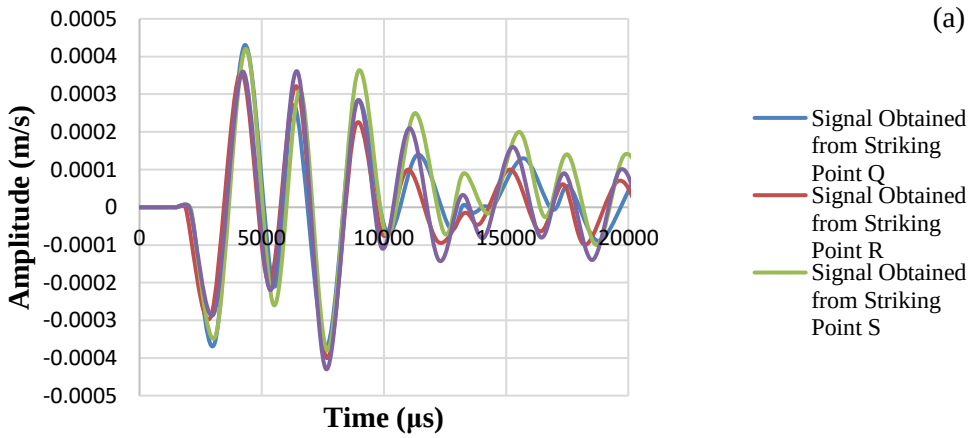

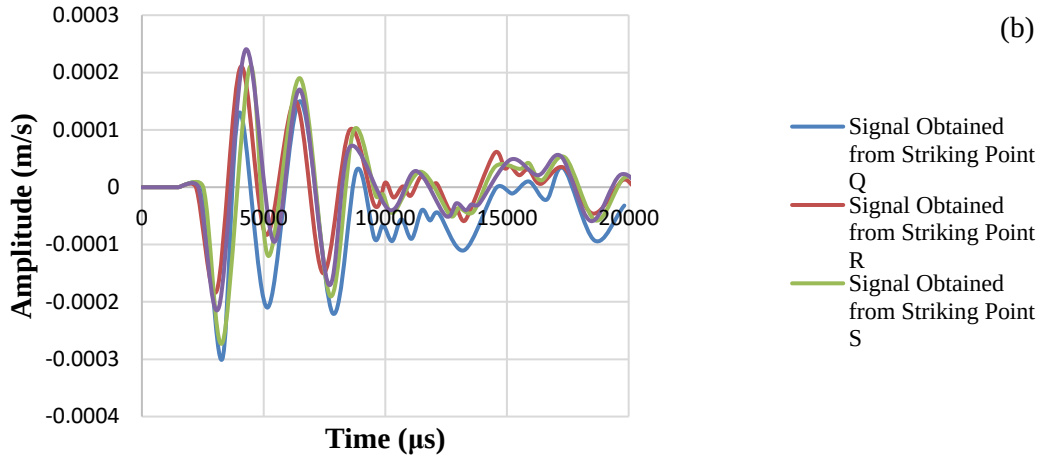

Fig. 13. Signals obtained from downward strikes on points Q to T for: a) Accelerometer 1 and b) Accelerometer 2

Table 7. Time lapses between the first four valleys for tests conducted by striking points Q to T

Striking point	Accelerometer	Δt_1 (µs)	Δt_2 (µs)	Δt_3 (µs)
Q	1	2420	2140	2500
	2	1860	2680	1720
R	1	2380	2360	2320
	2	2020	2340	2120
S	1	2380	2200	2420
	2	1880	2540	1880
T	1	2300	2280	2300
	2	2260	2260	2500
Average		2188	2350	2220

The results for conducted tests indicated in Tables 7 and 8 show that the average lapses between the impulse and the next valley are relatively close to each other. The time differences between the impulse and the next valley are summarized in Tables 9 and 10.

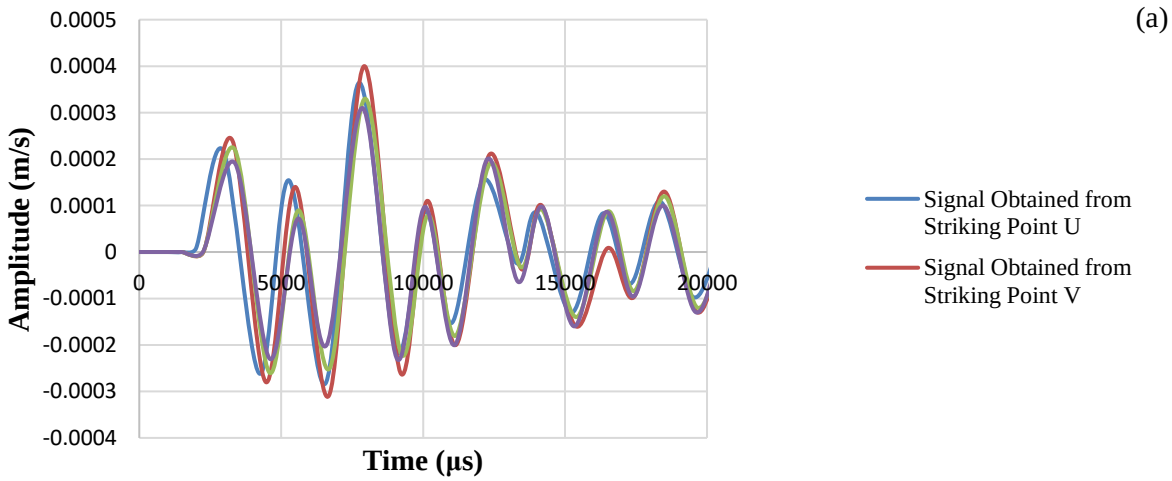

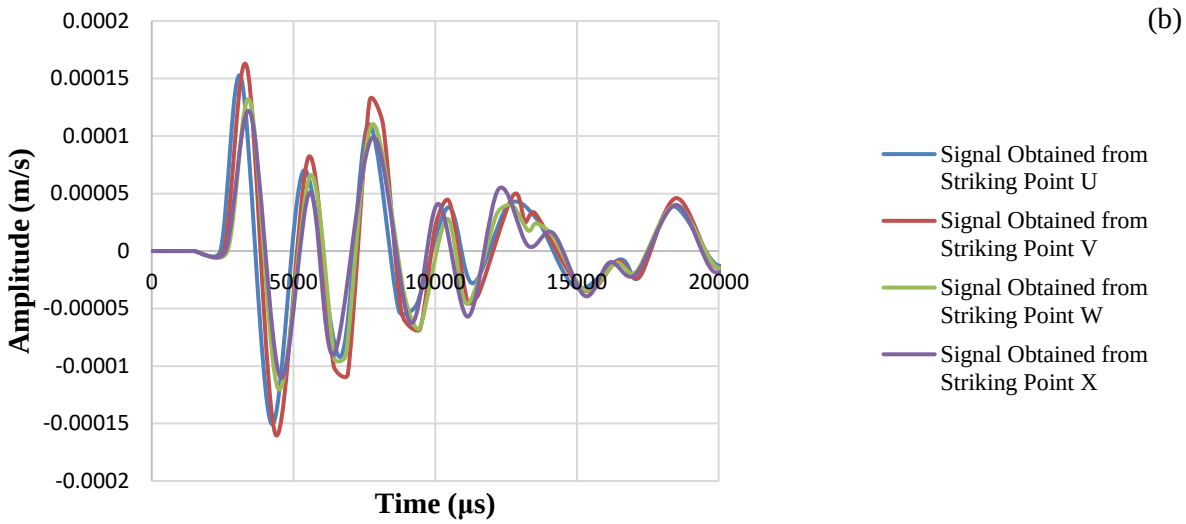

Fig. 14. Signals obtained from downward strikes on points U to X for: a) Accelerometer 1 and b) Accelerometer 2

Table 8. Time lapses between the first four valleys for tests conducted by striking points U to X

Striking point	Accelerometer	Δt_1 (μs)	Δt_2 (μs)	Δt_3 (μs)
U	1	2300	2480	2340
	2	2200	2280	2820
V	1	2220	2420	2220
	2	2180	2140	2320
W	1	2240	2340	2220
	2	2140	2160	2640
X	1	2220	2260	2200
	2	2100	2220	2300
Average		2200	2288	2383

Table 9. Time difference between the impulse and first valley for tests conducted by striking points Q to T

Striking point	Accelerometer	Δt_1 (μs)	Time lapse between accelerometers 1 and 2 (μs)
Q	1	2420	560
	2	1860	
R	1	2380	360
	2	2020	
S	1	2380	500
	2	1880	
T	1	2300	40
	2	2260	

Table 10. Time difference between the impulse and first valley for tests conducted by striking points U to X

Test	Accelerometer	Δt_1 (μs)	Time lapse between accelerometers 1 and 2 (μs)
U	1	2300	100
	2	2200	
V	1	2220	40
	2	2180	
W	1	2240	100
	2	2140	
X	1	2220	120
	2	2100	

The results indicated in Tables 9 and 10 show that the time lapses between accelerometers 1 and 2 are still smaller than 692 μs (2×1.5/4337 μs) particularly for the tests conducted using upward strike. It should be noted that the distance between the two accelerometers in this pile is 1.5m. Therefore, the first valleys followed by the impulses do not show reflections from the pile toe. In addition, the location and direction of the strikes do not affect the results. The results also show that the durations of the consecutive vibrations are very close to each other. For tests conducted by striking points Q to T, the average of second and third vibrations are only 7.4 and 1.5% smaller than the average duration of the first vibration respectively. For tests conducted on points U to X, the average of second and third vibrations are only 4 and 8.3% smaller than the average duration of the first vibration respectively. Therefore, the periods of vibrations in both conducted on points Q to T and U to X are relatively close together and a monotonic vibration occurs in both cases. These results support the conclusion that the signals received by the accelerometers contain echoes from unwanted sources that are distinctive from the echoes transmitted from the pile toe.

Complementary Discussion

In order to distinguish accurate results from inaccurate results, examples of successful SE tests which were previously conducted on a wood pile at another site (Rashidyan et al., 2016), are mentioned here. The street view and investigated pile are indicated in Figure 15. The investigated pile is one of the piles carrying a railway bridge. Two accurate examples of obtained signals from SE tests are indicated in Figure 16.

Fig. 15. Street view of bridge with superstructure and investigated pile

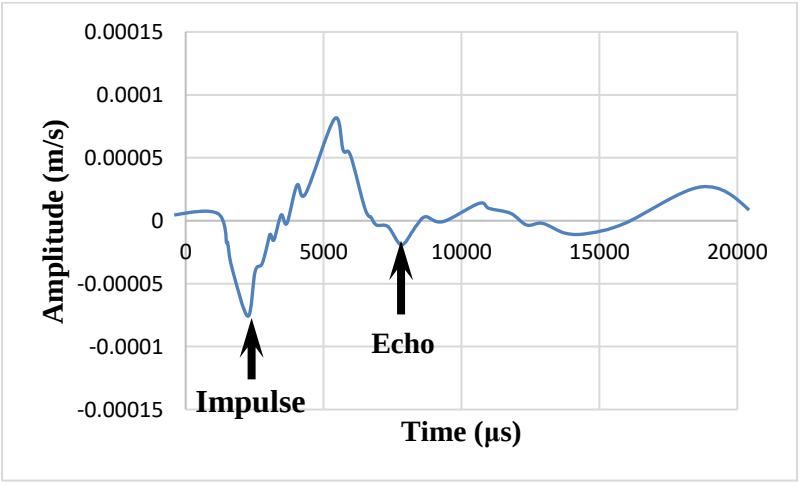

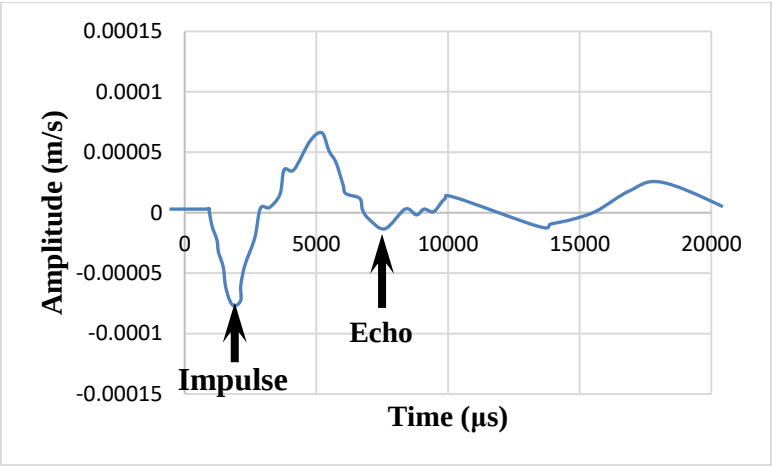

Fig. 16. Velocity signals obtained from conducting SE tests on the pile indicating in Figure 15 (Rashidyan et al., 2016)

Signals indicated in Figure 16 show clear impulses and the pile toe's echoes. No unusually undamped vibrations exist on these graphs, contrary to unusual vibrations which were previously observed in the dismantled bridge (see Figures 8 to 14).

It should be noted that the pile indicated in Figure 15 is different from the piles in the dismantled bridge in terms of their lateral stiffness. Since approximately 2.2 m laterally unbraced portion of the dismantled bridge's foundation was exposed, the lateral stiffness of the foundation was small. Thus, notably strong shakings were observed during striking on the foundation. It is probable that the intense shakings have been sensed by the accelerometers instead of the echoes from the pile toe. Such intense vibrations may prevent identifying the echoes from the pile bottom. Such difficulties have not been previously reported by the researchers since the SE method has traditionally been used for quality control of the piles, accompanied by a drilled shaft with an accessible top and piles underneath bridge decks. In the former, the drilled shaft is approximately buried in the ground and consequently will not experience such unbraced lateral vibrations. In the latter, however, the presence of the heavy superstructure such as the one indicated in Figure 15 can provide a significant lateral stiffness which prevents lateral shakings of the foundation.

Another source of difficulty can be the poor quality of the pile-pile cap connections. Since the dismantled bridge was old, the piles and the pile cap were deformed, and distorted. A poor and incomplete pile-pile cap connection example is shown in Figure 17. A full contact between the pile top surface and the bottom surface of the pile did not exist. They were in contact partially. It was expected that the multiple detachments between the pile and pile cap occurred at the time of striking and consequently made the wave propagation more complicated. Such detachments could be detected by the sensors which might have affected the obtained signals.

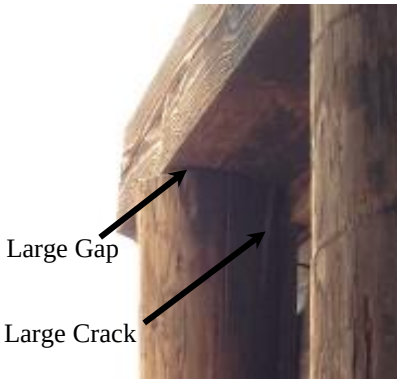

Fig. 17. Poor and incomplete pile-pile cap connection example

CONCLUSIONS

In this study, the performance of the SE tests in determining the depth of foundations which are comprised of piles and pile caps in the absence of superstructure is investigated. The investigated unknown bridge foundation in this case study had previously supported a bridge deck. However, at the time of testing, only the foundation comprising pile caps and piles were available. The bridge deck had previously been removed, since the bridge was going to be demolished. Many SE tests were performed on three piles of this foundation to evaluate the performance of SE testing method on such dismantled foundations. The velocity signals obtained from the accelerometers were investigated to measure the buried length of the piles.

The results showed that although clear valleys were recognizable after impulse, they were not the echoes from the pile toe. The results showed that the time lapses between the impulse and the next valley were approximately the same for both the accelerometers. This was an unexpected observation since the accelerometers were far from each other for 1.5 to 1.8 m. Therefore, the hypothesis was that different notable time lapses from the accelerometers would occur.

In addition, the presence of consecutive valleys with large amplitudes and non-decaying trends showed that the identified echoes were from other sources other than pile toes. Such vibrations may relate to the intense lateral vibrations of the foundation. The foundation was unbraced above ground and intense lateral vibrations was probable due to the low lateral stiffness. In addition, detachment of the pile cap from the pile during striking might be another reason for unsuccessful SE tests. It should be mentioned that poor connections between the deformed piles and pile cap were recognizable in this foundation.

In summary, the SE testing method does not seem to be a proper method to evaluate the condition of dismantled foundations comprising old unbraced wood piles that are poorly connected to the pile caps.

ACKNOWLEDGEMENT

This study is partially supported by the New Mexico Department of Transportation. The authors would like to thank Ms. Michelle Mann, Mr. Jeff Vigil, Mr. James Castillo (New Mexico Department of Transportation) and Dr. Thiet Nguen (Federal Highway Administration) for their valuable suggestions.

FUNDING

This work was supported by the New Mexico Department of Transportation (NMDOT) in cooperation with Federal Highway Administration (FHWA).

REFERENCES

American Concrete Institution. (2013). *Report on nondestructive test methods for evaluation of concrete in structures*, Farmington Hills, MI, United States.

American Society for Testing Materials. (2013). *Standard test method for low strain impact integrity testing of deep foundations*, West Conshohocken, PA, United States.

American Wood Council. (2018). *National design specification for wood construction*, Leesburg, VA, United States.

Briaud, J.-L., Ballouz, M. and Nasr, G. (2002). "Defect and length predictions by NDT methods for nine bored piles", *International Perspective on Theory, Design, Construction, and Performance*, 173-192.

Chai, H.-Y. and Phoon, K.-K. (2012). "Detection of shallow anomalies in pile integrity testing", *International Journal of Geomechanics*, 13(5), 672-677.

Chidambarathanu, N. (2019). "Processing digital image for measurement of crack dimensions in concrete", *Civil Engineering Infrastructures Journal*, 52(1), 11-22.

Davis, A.G. (1995). "Nondestructive evaluation of existing deep foundations", *Journal of Performance of Constructed Facilities*, 9(1), 57-

74.

Ghasemzadeh, H. and Abounouri, A.A. (2013). "The effect of dynamic permeability on velocity and intrinsic attenuation of compressional waves in sand", *Civil Engineering Infrastructures Journal*, 46(2), 221-231.

Hertlein, B. and Davis, A. (2007). *Nondestructive testing of deep foundations*, John Wiley & Sons.

Huang, D. and Chen, L. (2007). "Studies on parallel seismic testing for integrity of cemented soil columns", *Journal of Zhejiang University-Science A*, 8(11), 1746-1753.

Kramer, S. (1996). *Geotechnical earthquake engineering*, Pearson, London, England.

Lai, J., Yang, S.-T. and Chang, T.-S. (2012). "Evaluating the height of cantilever earth retaining walls by sonic echo non-destructive testing method", *International Journal of Applied Science and Engineering*, 10(2), 145-154.

Rashidyan, S., Ng, T. and Maji, A. (2016). "Bridge foundation depth estimation using Sonic Echo test", *In Experimental and Applied Mechanics*, Vol. 4, C. Sciammarella, J. Considine, and P. Gloeckner, (eds.), Springer International Publishing, pp. 99-106.

Rashidyan, S., Ng, T. and Maji, A. (2017). "Estimating the depth of concrete pier wall bridge foundations using nondestructive Sonic Echo", *Journal of Nondestructive Evaluation*, 36(3), 56.

Rashidyan, S., Ng, T. and Maji, A. (2019). "Practical aspects of nondestructive induction field testing in determining the depth of steel and reinforced concrete foundations", *Journal of Nondestructive Evaluation*, 38(1), 19.

Rausche, F. and Goble, G.G. (1979). Determination of pile damage by top measurements, *In Behavior of Deep Foundations, ASTM STP 670,* Raymo Lundgren, (ed.), American Society for Testing and Materials, pp. 500-506.

United States Department of Agriculture Forest Service (2010). *Wood handbook, wood as an engineering material*, Madison, Wisconsin, United States.

Weltman, A.J. (1977). *Integrity testing of piles: A review*, Construction Industry Research and Information Association, London, England.

White, B., Nagy, M. and Allin, R. (2008). "Comparing cross-hole sonic logging and low-strain integrity testing results", *In Proceedings of the Eighth International Conference on the Application of Stress Wave Theory to Piles*, pp. 471-476. Lisbon, Portugal.